C−H Bond Activation of Benzene by Unsaturated η²-Cyclopropene and η²-Benzyne Complexes of Niobium

Cédric Boulho,[†,‡] Pascal Oulié,[†,‡] Laure Vendier,[†,‡] Michel Etienne,*[,†,‡]
Véronique Pimienta,[⊥] Abel Locati,[§] Fabienne Bessac,[§] Feliu Maseras,*[,§,ǁ]
Dimitrios A. Pantazis,[#] and John E. McGrady*[,#]

*CNRS, Laboratoire de Chimie de Coordination (LCC), 205 Route de Narbonne,
F-31077 Toulouse, France, Université de Toulouse, UPS, INPT, LCC, F-31077 Toulouse, France,
Université de Toulouse, UPS, IMRCP, 118 Route de Narbonne, F-31062 Toulouse, France,
Institute of Chemical Research of Catalonia (ICIQ), Avgda. Països Catalans 16,
43007 Tarragona, Spain, Unitat de Química Física, Edifici Cn, Universitat Autònoma de
Barcelona, 08193 Bellaterra, Catalonia, Spain, and Department of Chemistry, Inorganic Chemistry
Laboratory, University of Oxford, South Parks Road, Oxford OX1 3QR, United Kingdom*

Received July 12, 2010; E-mail: michel.etienne@lcc-toulouse.fr (M.E.); fmaseras@iciq.es (F.M.);
john.mcgrady@chem.ox.ac.uk (J.E.M.)

Abstract: We report the synthesis of a niobium cyclopropyl complex, Tp^Me2^NbMe(c-C_3H_5)(MeCCMe), and show that thermal loss of methane from this compound generates an intermediate that is capable of activating both aliphatic and aromatic C−H bonds. Isotopic labeling, trapping studies, a detailed kinetic analysis, and density functional theory all suggest that the active intermediate is an η²-cyclopropene complex formed via β-hydrogen abstraction rather than an isomeric cyclopropylidene species. C−H activation chemistry of this type represents a rather unusual reactivity pattern for η²-alkene complexes but is favored in this case by the strain in the C_3 ring which prevents the decomposition of the key intermediate via loss of cyclopropene.

Introduction

The controlled activation of relatively inert C−H bonds by transition metal complexes remains one of the most important targets for the organometallic chemistry community.[1] The realization of this goal will, ultimately, require the design of systems capable of generating electron-deficient intermediates that are stable enough to be formed in significant concentrations yet at the same time reactive enough to cleave an extremely strong C−H σ bond. Controlling this delicate balance requires a detailed understanding of the factors that determine stability and reactivity in unsaturated intermediates.

The reactivity of β-hydrogens has long been acknowledged as the kinetic Achille's heel of transition metal alkyl complexes,

and the β-H elimination processes that yield alkene hydride complexes are now quite well understood.[2] Alternatively, β-H abstraction in dialkyl transition metal complexes L_nMR_2 leads to release of an alkane and formation of reduced alkene complexes L_nM(alkene). Such species can occasionally be trapped by a 2e-donor ligand, L, but are generally highly unstable with respect to alkene loss,[3,4] although notable exceptions are known with early transition metals that are good π-bases.[5] In contrast, alkyl phenyl or diphenyl complexes L_nMR(Ph) readily eliminate an alkane or benzene, respectively, to yield relatively stable benzyne complexes,[6,7] and a rich insertion chemistry has been developed.[8] Moreover, intermolecular C−H bond activation of various hydrocarbons by these unsaturated benzyne intermediates (a 1,3-addition of the C−H

---

† LCC, Toulouse.
‡ Université de Toulouse.
⊥ IMRCP, Toulouse.
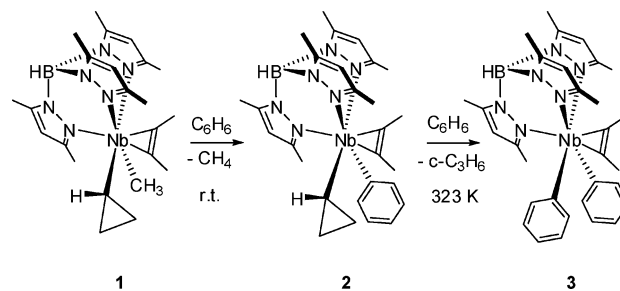§ ICIQ, Tarragona.
ǁ UAB, Barcelona.
ICL, Oxford.
(1) (a) See Special Issue of *Chemical Reviews* on "Selective Functionalization of C-H Bonds"; Crabtree, R. H. *Chem. Rev.* **2010**, *110*, 575. (b) Jazzar, R.; Hitce, J.; Renaudat, A.; Sofack-Freutzer, J.; Baudoin, O. *Chem.—Eur. J.* **2010**, *16*, 2654. (c) Balcells, D.; Clot, E.; Eisenstein, O. *Chem. Rev.* **2009**, *110*, 749. (d) Vastine, B. A.; Hall, M. B. *Coord. Chem. Rev.* **2009**, *253*, 1202. (e) Bergman, R. G. *Nature* **2007**, *446*, 391. (f) Perutz, R. N.; Sabo-Etienne, S. *Angew. Chem., Int. Ed.* **2007**, *46*, 2578. (g) Jones, W. D. *Inorg. Chem.* **2005**, *44*, 4475. (h) Lersch, M.; Tilset, M. *Chem. Rev.* **2005**, *105*, 2471. (i) Goldberg, K. I.; Goldman, A. S., Eds.; *Activation and Functionalization of C-H Bonds; ACS Symposium Series 885*; American Chemical Society: Washington, DC, 2004. (j) Labinger, J. A.; Bercaw, J. E. *Nature* **2002**, *417*, 507. (k) Arakawa, H.; et al. *Chem. Rev.* **2001**, *101*, 953. (l) Crabtree, R. H. *J. Chem. Soc., Dalton Trans.* **2001**, 2437.

(2) (a) Crabtree, R. *The Organometallic Chemistry of the Transition Metals*, 4th ed.; Wiley: Hoboken, 2005. (b) Elschenbroich, C. *Organometallics*, 3rd ed.; Wiley: Weinheim, 2006.
(3) (a) Negishi, E.; Cederbaum, F. E.; Takahashi, T. *Tetrahedron Lett.* **1986**, *27*, 2829. (b) Buchwald, S. L.; Watson, B. T.; Huffman, J. C. *J. Am. Chem. Soc.* **1987**, *109*, 2544. (c) Wang, S.-Y.; Abboud, K. A.; Boncella, J. M. *J. Am. Chem. Soc.* **1997**, *119*, 11990.
(4) b-H elimination and b-H abstraction pathways can be competitive, see: Wang, S.-Y.; Abboud, K. A.; Boncella, J. M. *Polyhedron* **2004**, *23*, 2733.
(5) (a) Freundlich, J. S.; Schrock, R. R.; Davis, W. M. *J. Am. Chem. Soc.* **1996**, *118*, 3643. (b) Baumann, R.; Stumpf, R.; Davis, W. M.; Liang, L.-C.; Schrock, R. R. *J. Am. Chem. Soc.* **1999**, *121*, 782.
(6) (a) Erker, G. *J. Organomet. Chem.* **1977**, *134*, 189. (b) Cockcroft, J. K.; Gibson, V. C.; Howard, A. K.; Poole, A. D.; Siemeling, U.; Wilson, C. *J. Chem. Soc., Chem. Commun.* **1992**, 1668. (c) McLain, S. J.; Schrock, R. R.; Sharp, P. R.; Churchill, M. R.; Youngs, W. J. *J. Am. Chem. Soc.* **1979**, *101*, 263. (d) Buijink, J. K. F.; Kloetstra, K. R.; Meetsma, A.; Teuben, J. H.; Smeets, W. J. J.; Spek, A. L. *Organometallics* **1996**, *15*, 2523.

bond across a M-benzyne bond) has also been achieved, indicating that β-H abstraction can in certain circumstances be reversible.[6a,7,9] Analogous β-H abstraction with other unsaturated ligands, for example, η^3-allyl alkyl and vinyl alkyl complexes of molybdenum and tungsten, generate unsaturated η^2-allene,[10] η^2-diene,[11] or η^2-alkyne[12] complexes that are able to cleave C−H bonds of various hydrocarbons. In the case of unsaturated η^2-alkene complexes,[13,14] however, this fundamentally important C−H activation event remains exceedingly rare.

In contrast to the general instability of the unsaturated alkene species arising from β-H abstraction, the corresponding alkylidene complexes formed by α-H abstraction reactions in dialkyl complexes of the group 5 metals (typically those devoid of β-hydrogens) are rather stable.[15] Moreover, in the absence of suitable stabilizing agents, activation of the C−H bonds of hydrocarbons (a 1,2-addition of the C−H bond across a M=C bond) by unsaturated alkylidenes appears to be relatively commonplace.[9a,16] Very recently, related α-H abstractions from alkyl alkylidene titanium complexes have also yielded reactive alkylidyne complexes that activate various hydrocarbon C−H bonds (a 1,2-addition of the C−H bond across a Ti≡C bond).[17] Thus, in general C−H bond activation pathways that are zero order in hydrocarbon tend to follow α-H abstraction/1,2-C-H

(7) Late transition metal benzyne complexes, that also activate XH bonds of various substrates, are formed via a different pathway; see: (a) Hartwig, J. F.; Bergman, R. G.; Andersen, R. A. *J. Am. Chem. Soc.* **1991**, *113*, 3403. (b) Hartwig, J. F.; Andersen, R. A.; Bergman, R. G. *J. Am. Chem. Soc.* **1989**, *111*, 2717.

(8) (a) Buchwald, S. L.; Nielsen, R. B. *Chem. Rev.* **1988**, *88*, 1047. (b) Negishi, E.; Takahashi, T. *Acc. Chem. Res.* **1994**, *27*, 124.

(9) (a) Wada, K.; Pamplin, C. B.; Legzdins, P.; Patrick, B. O.; Tsyba, I.; Bau, R. *J. Am. Chem. Soc.* **2003**, *125*, 7035. (b) Wada, K.; Pamplin, C. B.; Legzdins, P. *J. Am. Chem. Soc.* **2002**, *124*, 9680. (c) Pamplin, C. B.; Legzdins, P. *Acc. Chem. Res.* **2003**, *36*, 223. (d) Fagan, P. J.; Manriquez, J. M.; Maatta, E. A.; Seyam, A. M.; Marks, T. J. *J. Am. Chem. Soc.* **1981**, *103*, 6650.

(10) (a) Ng, S. H. K.; Adams, C. S.; Legzdins, P. *J. Am. Chem. Soc.* **2002**, *124*, 9380. (b) Ng, S. H. K.; Adams, C. S.; Hayton, T. W.; Legzdins, P.; Patrick, B. O. *J. Am. Chem. Soc.* **2003**, *125*, 15210.

(11) (a) Tsang, J. Y. K.; Buschhaus, M. S. A.; Legzdins, P. *J. Am. Chem. Soc.* **2007**, *129*, 5372. (b) Tsang, J. Y. K.; Buschhaus, M. S. A.; Graham, P. M.; Semiao, C. J.; Semproni, S. P.; Kim, S. J.; Legzdins, P. *J. Am. Chem. Soc.* **2008**, *130*, 3652.

(12) (a) Debad, J. D.; Legzdins, P.; Lumb, S. A.; Batchelor, R. J.; Einstein, F. W. B. *J. Am. Chem. Soc.* **1995**, *117*, 3288. (b) Debad, D.; Legzdins, P.; Lumb, S. A.; Rettig, S. J.; Batchelor, R. J.; Einstein, F. W. B. *Organometallics* **1999**, *18*, 3414. (c) Legzdins, P.; Lumb, S. A. *Organometallics* **1997**, *16*, 1825–1827.

(13) Buchwald, S. L.; Kreutzer, K. A.; Fisher, R. A. *J. Am. Chem. Soc.* **1990**, *112*, 4600.

(14) "Protonolysis" of η^2-alkene complexes occurs readily with the more reactive alkyne C-H bonds to give alkynyl complexes; see for example: (a) Cohen, S. A.; Bercaw, J. E. *Organometallics* **1985**, *4*, 1006. (b) Kissounko, D.; Epshteyn, A.; Fettinger, J. C.; Sita, L. R. *Organometallics* **2006**, *25*, 531.

(15) (a) Schrock, R. R. *Acc. Chem. Res.* **1979**, *12*, 98. (b) Schrock, R. R. *J. Am. Chem. Soc.* **1974**, *96*, 6796.

(16) (a) van der Heiden, H.; Hessen, B. *J. Chem. Soc., Chem. Commun.* **1995**, 145. (b) Coles, M. P.; Gibson, V. C.; Clegg, W.; Elsegood, M. R.; Porelli, P. A. *J. Chem. Soc., Chem. Commun.* **1996**, 1963. (c) Tran, E.; Legzdins, P. *J. Am. Chem. Soc.* **1997**, *119*, 5071. (d) Cheon, J.; Rogers, D. M.; Girolami, G. S. *J. Am. Chem. Soc.* **1997**, *119*, 6804. (e) Adams, C. S.; Legzdins, P.; Tran, E. *J. Am. Chem. Soc.* **2001**, *123*, 612. (f) Adams, C. S.; Legzdins, P.; Tran, E. *Organometallics* **2002**, *21*, 1474. (g) Wada, K.; Pamplin, C. B.; Legzdins, P. *J. Am. Chem. Soc.* **2002**, *124*, 9680. (h) Adams, C. S.; Legzdins, P.; McNeil, W. S. *Organometallics* **2001**, *20*, 4939.

(17) (a) Bailey, B. C.; Fan, H.; Baum, E. W.; Huffman, J. C.; Baik, M.-H.; Mindiola, D. J. *J. Am. Chem. Soc.* **2005**, *127*, 16016. (b) Bailey, B. C.; Fan, H.; Huffman, J. C.; Baik, M.-H.; Mindiola, D. J. *J. Am. Chem. Soc.* **2006**, *128*, 6798. (c) Bailey, B. C.; Huffman, J. C.; Mindiola, D. J. *J. Am. Chem. Soc.* **2007**, *129*, 5302. (d) Bailey, B. C.; Fan, H. J. J.; Huffman, J. C.; Baik, M.-H.; Mindiola, D. J. *J. Am. Chem. Soc.* **2007**, *129*, 8781.

Scheme 1

bond addition sequences rather than the β-H abstraction/1,3-C-H addition alternative unless unsaturated benzyne, alkyne, or allene intermediates can be generated.

In this paper, we show that a transient η^2-cyclopropene niobium complex formed by β-H abstraction from an α-CC agostic cyclopropyl methyl precursor[18] is capable of activating a C−H bond of benzene, generating a cyclopropyl phenyl complex. A second β-H abstraction process then generates an η^2-benzyne complex that can activate a C−H bond of a second benzene molecule to generate the diphenyl species. The transient intermediates, an η^2-cyclopropene and an η^2-benzyne, are generated under remarkably mild conditions and both have been trapped by Lewis bases. In addition, we report a detailed kinetic analysis of the C−H activation reactions. Finally, we use density functional theory to explore the corresponding potential energy surface - the effectiveness of a joint experimental and theoretical approach to mechanistic problems such as this has been amply demonstrated by a number of authors.[1c,19] Part of this work has previously been communicated.[20]

Results and Discussion

C−H Bond Activation of Benzene: Synthetic Aspects. As previously communicated,[20] the niobium cyclopropyl complex $Tp^{Me2}NbMe(c\text{-}C_3H_5)(MeCCMe)$ (**1**) reacts smoothly at room temperature with benzene ($t_{1/2}$ ca. 7 h) to give first methane and $Tp^{Me2}NbPh(c\text{-}C_3H_5)(MeCCMe)$ (**2**) and subsequently, over the course of ca. two days, cyclopropane and $Tp^{Me2}NbPh_2$-$(MeCCMe)$ (**3**) (Scheme 1). The sequence of reactions confirms that the Nb−Me bond in **1** is more reactive than the Nb-(c-C_3H_5) bond.

The initial step in the reaction sequence could, in principle, involve either β-H abstraction to form an intermediate alkene complex $Tp^{Me2}Nb(\eta^2\text{-}c\text{-}C_3H_4)(MeCCMe)$ (**A**) or, alternatively, α-H abstraction to form an alkylidene intermediate $Tp^{Me2}Nb$-$(=CC_2H_4)(MeCCMe)$ **A'**. To distinguish these two possibilities, **1** was reacted with benzene-d_6 in an NMR tube, at which point only CH_4 was observed. A single deuterium was found (^{1}H, ^{13}C, and ^{2}H NMR) on the β carbons of the cyclopropyl ring in $Tp^{Me2}Nb(C_6D_5)(c\text{-}C_3H_4D)(MeCCMe)$ **2-d_6** and, moreover, specifically on the same enantioface of the cyclopropyl ring as the niobium.[20,21] The two possible diastereomers of **2-d_6** were formed in a ca. 2:1 ratio as shown in Scheme 2. The fact that

(18) Boulho, C.; Keys, T.; Coppel, Y.; Vendier, L.; Etienne, M.; Locati, A.; Bessac, F.; Maseras, F.; Pantazis, D. A.; McGrady, J. E. *Organometallics* **2009**, *28*, 940.

(19) Selected recent reviews: (a) Boutadla, Y.; Davies, D. L.; Macgregor, S. A.; Poblador-Bahamonte, A. I. *Dalton Trans.* **2009**, 5820. (b) Lin, Z. *Acc. Chem. Res.* **2010**, *43*, 602. (c) Foley, N. A.; Lee, J. P.; Ke, Z.; Gunnoe, T. B.; Cundari, T. R. *Acc. Chem. Res.* **2009**, *42*, 585.

(20) Oulié, P.; Boulho, C.; Vendier, L.; Coppel, Y.; Etienne, M. *J. Am. Chem. Soc.* **2006**, *128*, 15962.

(21) Yin, J.; Jones, W. M. *Organometallics* **1993**, *12*, 2013.

Scheme 2

2-d₆, 2:1 ratio   *some* **2-d₇**
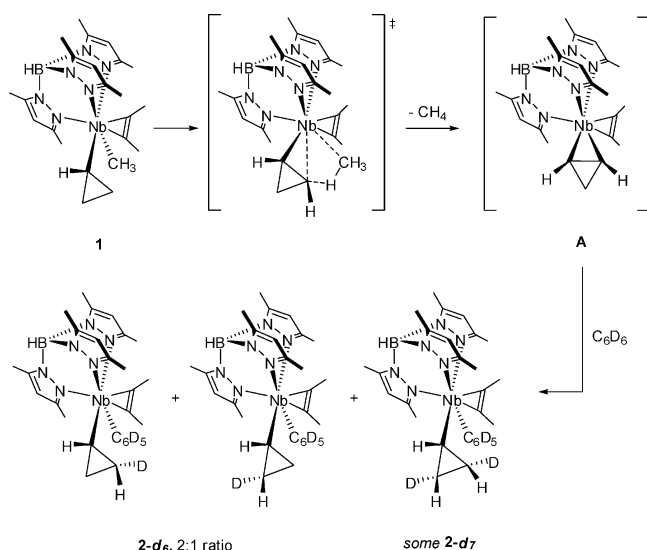
D is not observed at the α carbon confirms that α-H abstraction from **1** to yield a cylopropylidene intermediate **A'** is not operative here. Despite complications due to the competing reaction giving **3-d₁₀** (see below) and other decomposition pathways, careful monitoring of the spectra indicated that some dideuterated **2-d₇** was formed. Moreover, D was again found specifically on the β carbons and on the same enantioface as the niobium. This observation suggests that **2** can reversibly eliminate and re-add benzene, albeit very slowly. Overall these experiments show that **1** reacts with benzene to give **2** via a rate-determining methane loss (see kinetics below) that generates a transient and highly reactive unsaturated η²-cyclopropene intermediate **A**. A C−H bond of benzene then adds across an Nb−C bond of **A** to give **2**. The combined β-H abstraction/

1,3-C-H bond activation route is, as mentioned above, a very unusual mechanism[9] for early transition metal complexes.

Trapping of Unsaturated Intermediates. The unsaturated intermediate **A** (Scheme 3) has been characterized by a series of trapping experiments, and also by a detailed analysis of the kinetics of the reaction (vide infra).

The cyclopropene species **A** was trapped by mixing **1** with an excess of pyridine in pentane at room temperature, resulting in smooth conversion to methane and the air-sensitive η²-cyclopropene pyridine complex Tp^{Me2}Nb(c-C₃H₄)(NC₅H₅)-(MeCCMe) (**4**, Scheme 3). **4**, the only metal containing species identified, is a formally 18e niobium(I) complex although backbonding to the cyclopropene is clearly substantial. It is significant that no C−H bond of the heteroaromatic pyridine is activated under these conditions. Compound **4** crystallizes from the reaction mixture as a pyridine solvate, and the X-ray structure (Figure 1) confirms the presence of an η²-cyclopropene ligand. The alkyne and cyclopropene ligands are aligned parallel to the N(5)−Nb(1)−NC₅H₅ axis while the N-bound pyridine ligand lies in the wedge defined by the two cis pyrazolyl rings, and is coplanar with the trans pyrazolyl. The short niobium−alkyne carbon bond lengths (ca. 2.09 Å) and the long coordinated alkyne C'C bond (1.309(8) Å) are indicative of a four-electron-donor alkyne. The niobium to cyclopropene carbon bonds are longer (ca. 2.19 Å) and the long coordinated C=C bond (1.447(9) Å, only ca. 0.02 Å shorter than the two non-coordinated CC bonds) provides evidence of substantial back-bonding from the metal. In addition to pyridine signals, relevant NMR data for **4** include the ¹H NMR signals ascribed to the Nb-coordinated η²-C*H*=C*H*C*H*₂ at δ 2.83 (broad triplet, *J* 6.3 Hz) and 2.60 (an overlapping multiplet). The associated ¹³C NMR signals are observed as doublets at δ 74.5 (*J* 173 Hz) and 68.4 (*J* 168 Hz). The diastereotopic methylene group protons appear at δ 1.62 (pseudo quartet, *J* 5.4 Hz) and −0.20 (broad doublet, *J* 4.8 Hz) with the carbon resonating at δ 27.3 (dd, *J*

Scheme 3

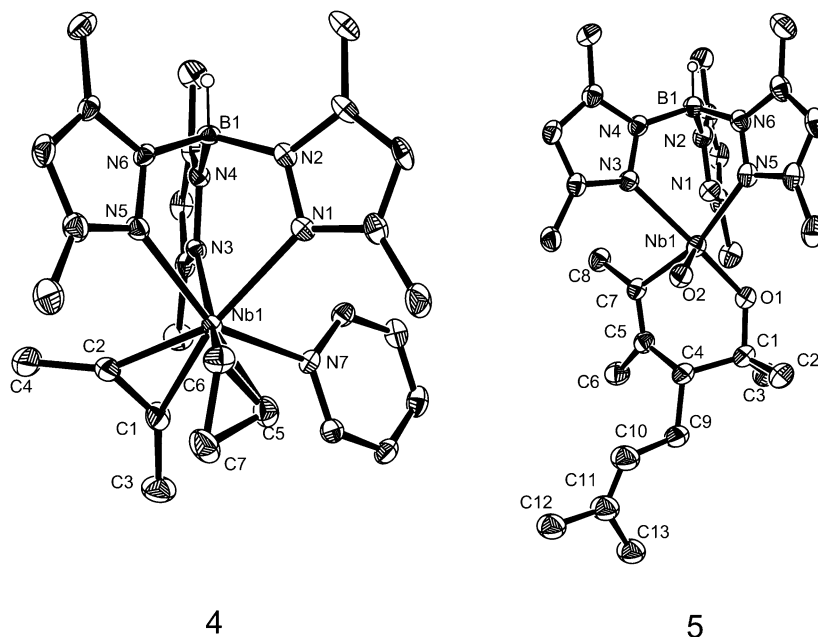4   5
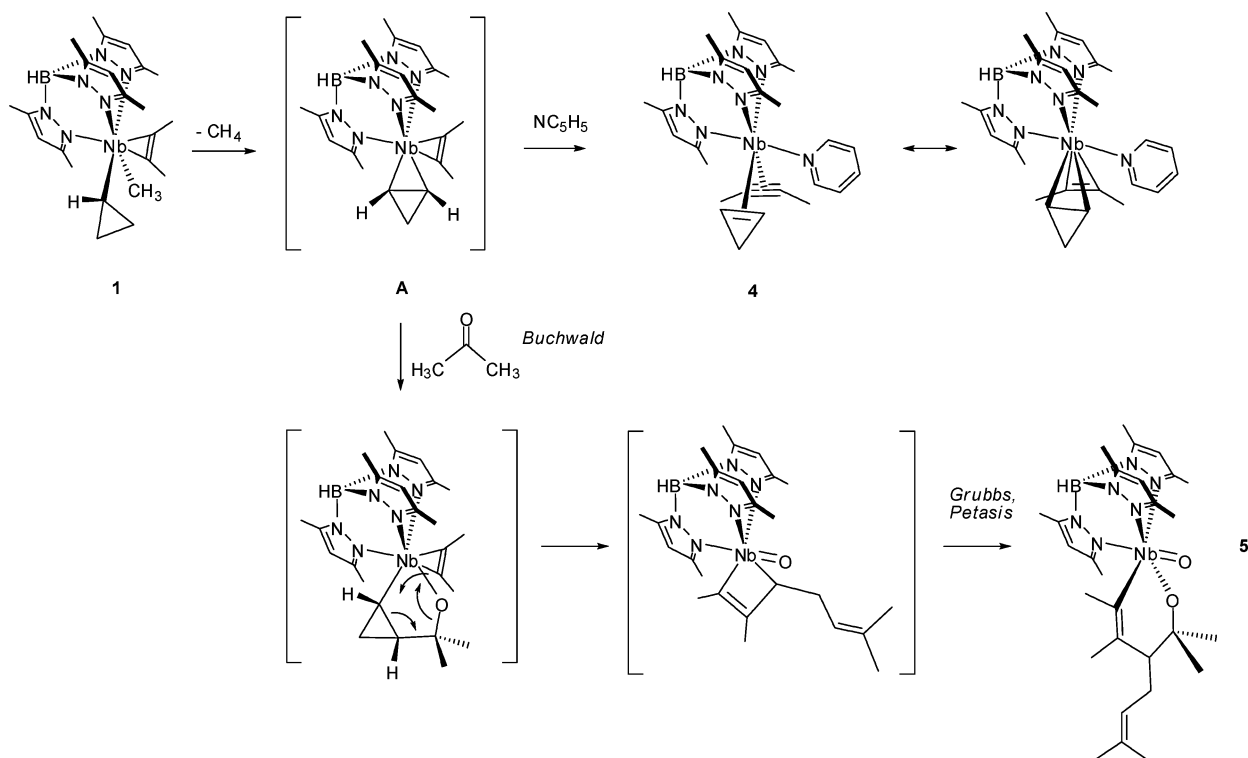
Figure 1. Plots of the X-ray molecular structure of Tp^{Me2}Nb(c-C$_3$H$_4$)(NC$_5$H$_5$)(MeCCMe) (**4**) and Tp^{Me2}NbO[CMeCMeCH(CH$_2$CH=CMe$_2$)CMe$_2$O] (**5**). Relevant bond lengths (Å) and angles (°): **4**: Nb(1)−C(1) 2.096(6), Nb(1)−C(2) 2.085(6), Nb(1)−C(5) 2.186(6), Nb(1)−C(6) 2.178(6), C(1)−C(2) 1.309(8), C(5)−C(6) 1.447(9), C(5)−C(7) 1.470(9), C(6)−C(7) 1.474(9), Nb(1)−N(7) 2.368(4); N(5)−Nb(1)−N(7) 149.98(16). **5**: Nb(1)−O(1) 1.895(3), Nb(1)−O(2) 1.709(3), C(1)−O(1) 1.437(5), C(1)−C(4) 1.576(7), C(4)−C(5) 1.541(6), C(5)−C(7) 1.349(6), C(4)−C(9) 1.541(6), C(9)−C(10) 1.429(7), C(10)−C(11) 1.305(7).

147, 174 Hz). The chemical shifts of the niobium-bound alkyne carbons (δ 209.1 and 206.9) also testify to the four-electron-donor behavior of the ligand.

Following precedents in zirconium chemistry where η^2-cycloalkene intermediates resulting from β-H abstraction were claimed, that is, from Cp$_2$ZrMe(c-C$_3$H$_5$)[8a] or indeed trapped from Cp$_2$ZrMe(c-C$_4$H$_7$),[22] we have also studied the reaction between **1** and acetone. We hoped to observe insertion chemistry in the Nb-(η^2-cyclopropene) framework (Scheme 3), but the outcome proved to be more complicated than initially anticipated. Simple inspection of the crude reaction mixture by ^{1}H NMR spectroscopy indicated the formation of a major metallacyclic oxo complex Tp^{Me2}NbO[CMeCMeCH(CH$_2$CH=CMe$_2$)CMe$_2$O] (**5**) together with other unidentified species. **5** results from the reaction of **1** with 2 equiv of acetone (Scheme 3). ^{1}H and ^{13}C NMR spectra (see Experimental Section) of **5** are fully interpretable when the X-ray crystal structure is known (Figure 1). The sequence of steps leading to **5** is not known, but the structure reveals that 1 equiv of acetone [O(1), C(1), C(2), C(3)] has inserted into a Nb−C bond of Nb-(η^2-cyclopropene). This has coupled with 2-butyne [C(5), C(6), C(7), C(8)] to give an unsaturated six-membered ring and the coordinated cyclopropene has been ring opened to generate a >CH−CH$_2$−CH= chain [C(4), C(9), C(10)]. Most remarkably, the C=O bond of a second equivalent of acetone has also been cleaved to give Nb=O and =CMe$_2$ units [C(11), C(12), C(13)]. When the trapping experiment was repeated with acetone-d_6, the signals for the four methyl groups coming from acetone [i.e., C(2), C(3), C(12), C(13)] were absent from the ^{1}H NMR spectrum of **5-d_{12}** confirming the assignment and ruling out the adventitious introduction of dioxygen in the reaction medium. Metallaoxacyclohexene structures similar to **5** have precedent in early transition metal chemistry and their formation gives clues to a possible mechanism of the trapping reaction. Thus, in one

possible route, shown in Scheme 3, the cyclopropene intermediate **A** is trapped by acetone leading to a oxacyclopentane intermediate. A similar zirconaoxacyclopentane product has been reported by Buchwald and co-workers in the reaction of Cp$_2$ZrMe(c-C$_3$H$_5$) with acetone, which proceeds via CH$_4$ loss to form [Cp$_2$Zr(c-C$_3$H$_4$)].[7a,22] The oxacyclopentane intermediate then undergoes ring-opening to form an oxacyclobutene species which can insert a second molecule of acetone to form **5**. Grubbs and Petasis have reported that titanaoxacyclohexenes with spectroscopic properties similar to **5** can be formed by the insertion of a ketone into the Ti−C single bond of titanocenecyclobutenes.[23] Thus, both insertion steps in Scheme 3 have precedents in the literature, leaving only the cyclopropyl ring-opening, Nb=O formation, and alkyl alkyne coupling to complete the process.

The second bond activation step shown in Scheme 1, leading from the phenyl cyclopropyl complex **2** and benzene to the diphenyl complex **3** and cyclopropane via intermediate **B**, occurs readily at higher temperatures, typically above 323 K (Scheme 4). We have been unable to trap **B** starting from **2**, although NMR data on reaction mixtures containing **2** and PMe$_3$ do suggest that a trapped product (**6**) was formed. However, the addition of excess PMe$_3$ to a solution of **3** in cyclohexane at 323 K gave Tp^{Me2}Nb(η^2-C$_6$H$_4$)(MeCCMe)(PMe$_3$) (**6**), confirming that C−H activation by intermediate **B** is also reversible. The product **6** was subsequently converted to the carbonyl derivative Tp^{Me2}Nb(η^2-C$_6$H$_4$)(MeCCMe)(CO) (**7**).

Broad ^{13}C NMR resonances for the four Nb bound alkyne carbons are observed for **6** between δ 207.0 (d, $^2J_{PC}$ 20 Hz), 202.5, 185.4 (d, $^2J_{PC}$ 30 Hz), 180.2 (MeC≡) and at higher field in **7**, δ 180.0, 177.3, 170.3, 166.6. Compound **7** has been characterized by X-ray crystallography (Figure 2): the benzyne and 2-butyne ligands lie approximately parallel to the Nb−CO

(22) Fischer, R. A.; Buchwald, S. L. *Organometallics* **1990**, *9*, 871.

(23) (a) Meinhart, J. D.; Grubbs, R. H. *Bull. Chem. Soc. Jpn.* **1988**, *61*, 171. (b) Petasis, N. A.; Fu, D.-K. *Organometallics* **1993**, *12*, 3776.

Scheme 4
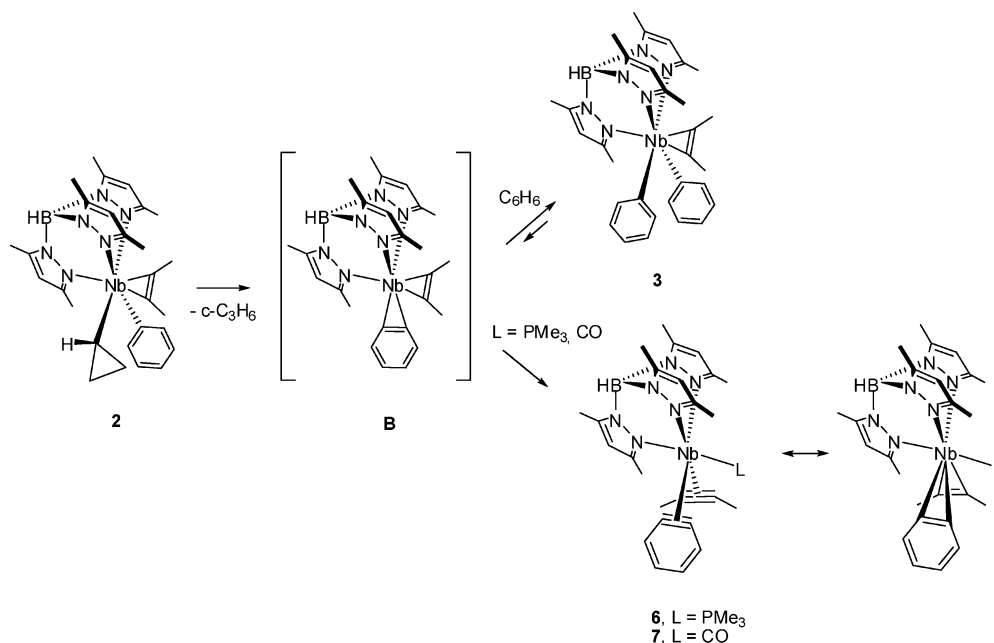
axis and the Nb–C bond is longer for the carbon proximal to CO. This feature has been observed previously in bis(alkyne) complexes such as $Tp^{Me2}Nb(PhCCMe)_2(CO)$.[24] A formal electron count of 18 in complex **7** requires donation of a total of six electrons from the alkyne and the benzyne, each of which can, in principle, donate a maximum of four.[25] Similar situations are common in carbonyl bis(alkyne) niobium(I) complexes, including $Tp^{Me2}Nb(PhCCMe)_2(CO)$, where each alkyne ligand is formally a three-electron donor. As the metric parameters for the Nb-alkyne and Nb-benzyne interactions in **7** are rather similar to those in $Tp^{Me2}Nb(PhCCMe)_2(CO)$, we propose that the benzyne ligand in the former is also a three-electron donor.
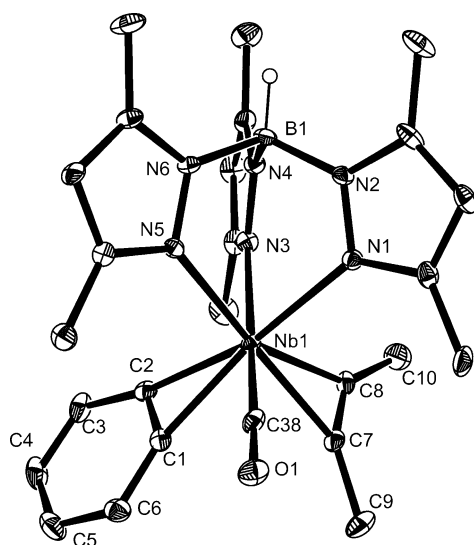

Figure 2. Plot of the X-ray molecular structure of $Tp^{Me2}Nb(\eta^2-C_6H_4)(MeCCMe)(CO)$ (**7**). Relevant bond lengths (Å) and angles (°): Nb(1)–C(1) 2.183(2), Nb(1)–C(2) 2.152(3), Nb(1)–C(7) 2.165(3), Nb(1)–C(8) 2.110(3), C(1)–C(2) 1.328(4), C(7)–C(8) 1.281(4), C(2)–C(3) 1.412(4), C(3)–C(4) 1.368(5), C(4)–C(5) 1.398(5), C(5)–C(6) 1.380(4), C(1)–C(6) 1.376(4), Nb(1)–C(38) 2.029(3), C(38)–O(1) 1.165(4); C(3)–C(2)–Nb(1) 168.4(3), C(6)–C(1)–Nb(1) 162.3(3), C(9)–C(7)–Nb(1) 145.5(2), C(10)–C(8)–Nb(1) 142.2(3).

Thus, although η^2-benzyne complexes such as **6** and **7** are well-known (including (2e)-niobium[6b] or (4e)-tantalum[6c] complexes), **6** and **7** appear to be the only examples in which a benzyne ligand behaves formally as a (3e)-donor.

Reaction Mechanism: Kinetic Aspects. In cyclohexane-d_{12}, the reaction converting **1** to **2** is first order in **1** and zeroth order in benzene ($k_{obs} = (2.93 \pm 0.05) \times 10^{-5}$ s^{-1} = $(1.76 \pm 0.03) \times 10^{-3}$ min^{-1}), and no isotope effect was seen when benzene-d_6 was activated in identical conditions ($k_H/k_D = 1.0$ at 303 K). Temperature-dependent studies yielded $\Delta H^{\ddagger} = (99 \pm 5)$ kJ/mol and $\Delta S^{\ddagger} = (-6 \pm 10)$ J/Kmol. These previously reported experiments provide further evidence that intramolecular loss of methane is the rate-determining step (Scheme 2).[20] Although intermediate **A** is generated in the rate-determining step, its subsequent reaction with benzene may still discriminate between the C–H and C–D bonds of benzene and benzene-d_6 in a competition experiment. Thus, a k_H/k_D of 4.0 ± 0.5 was measured for the reaction between **1** and an excess of a 1:1 molar mixture of benzene and benzene-d_6 forming **2** and **2-d_6** in cyclohexane at 310 K (analysis was done in dichloromethane-d_2 by ^{1}H NMR at 220 K). This experimental procedure was necessary for a reliable integration of the phenyl signals of **2** due to restricted rotation about the Nb–Ph bond and signal broadening. As has been discussed elsewhere,[17d,26] the interpretation of these kinetic isotope effects must be treated with some caution, because coordination of benzene to give a transient C–H σ complex, rather than cleavage of the C–H bond, may be rate limiting. Moreover, there are relatively few precedents on which to base the interpretation of k_H/k_D in hydrocarbyl complexes such as those of interest here. For example, the unsaturated titanium alkylidyne (PNP)Ti≡C-t-Bu (PNP = N[C$_6$H$_3$-2-P(i-Pr)$_2$-4-Me]$_2$) generated via α-H abstraction of neopentane from (PNP)Ti(=CH-t-Bu)(CH$_2$-tBu), adds a benzene C–H bond across the polarized Ti≡C linkage to give

(24) Lorente, P.; Etienne, M.; Donnadieu, B. *An. Quim. Int. Ed.* **1996**, *92*, 88, and references therein.
(25) Templeton, J. L. *Adv. Organomet. Chem.* **1989**, *89*, 1.
(26) (a) Jones, W. D.; Feher, F. J. *J. Am. Chem. Soc.* **1986**, *108*, 4814. (b) Jones, W. D. *Acc. Chem. Res.* **2003**, *36*, 140.
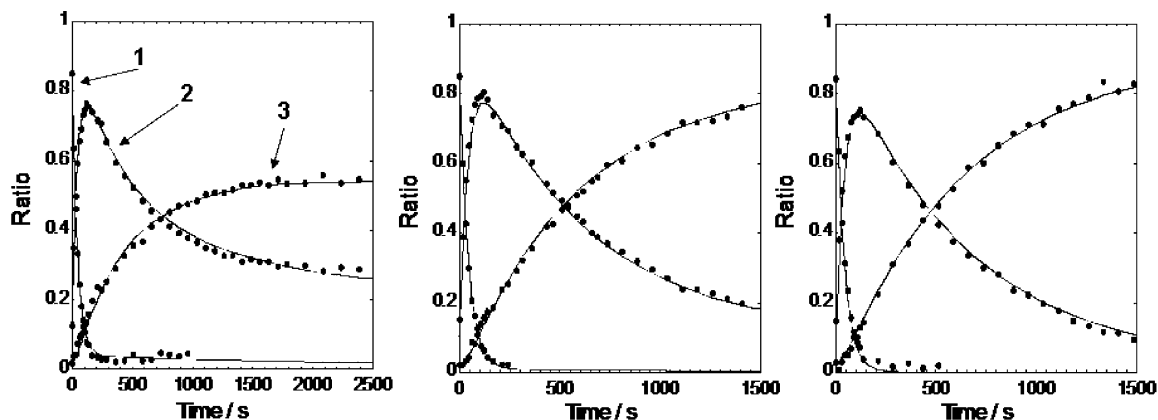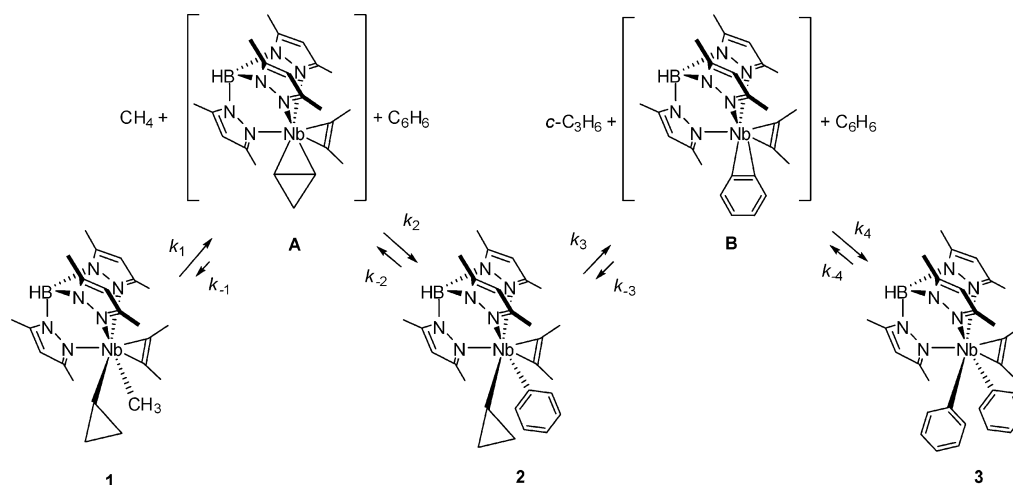
Figure 3. Experimental (°°°) and simulated (--) reaction profiles for the reaction of **1** with C_6H_6 giving **2** then **3** (^1H NMR, cyclohexane-d_{12}, 323 K, from left to right: $[C_6H_6]/[1] = 2, 6, 31$).

Scheme 5

(PNP)Ti(=CH-*t*-Bu)(Ph). The C−H activation step shows a moderate intramolecular isotope effect $k_H/k_D = 1.33$ with 1,3,5-$C_6H_3D_3$ or 1.03 when a 1:1 mixture of benzene and benzene-d_6 is used. Calculations in this case suggest that a C−H σ, rather than C=C π, complex is formed between benzene and the unsaturated metal complex.[17d] Similarly, the unsaturated tungsten neopentylidene Cp*W(NO)(=CH-*t*-Bu), generated from Cp*W(NO)(CH$_2$-*t*-Bu)$_2$, activates the C−H/D bonds of benzene/benzene-d_6 and tetramethylsilane/tetramethylsilane-d_{12} with k_H/k_D values of 1.03 and 1.07, respectively. On this basis, coordination of a C−H or C=C bond was proposed to be rate limiting.[16e] In contrast, an isotope effect k_H/k_D of 4.3 has been measured for the oxidative cleavage of CH$_2$D$_2$ by Tp^{Me2}Rh(CNCH$_2$-*t*-Bu) via an intermediate σ-CH$_4$ complex.[27] On the basis of the magnitude of the isotope effect in the present case, we are confident that it reflects a C−H/C−D bond cleavage event, with significant weakening of the bonds in the transition state.

Attempts to study the kinetics of the second activation of benzene (**2** → **3** via intermediate **B**) by conventional methods were frustrated by the reversibility of several steps. We therefore resorted to numerical simulation to analyze the experimental data acquired by ^1H NMR; similar procedures have been applied with some success in the study of intricate reaction mechanisms

in organometallic chemistry[28] and other complex systems.[29] We conducted three separate experiments adding 2, 6, and 31 equiv of benzene to solutions of **1** in cyclohexane-d_{12} at 323 K. The concentrations of **1**, **2**, and **3** as determined by integration of key ^1H NMR signals are shown as a function of time in Figure 3. In each case, rapid disappearance of **1** and build up of intermediate **2** is followed by a rather slower conversion of **2** to **3**. The kinetic model shown in Scheme 5, involving eight distinct processes, was used to simultaneously fit the three sets of data (full details are given in the Supporting Information).[30]

It is important to emphasize that because we are unable to measure the concentrations of intermediates **A** and **B**, we are

(27) Northcutt, T. O.; Wick, D. D.; Vetter, A. J.; Jones, W. D. *J. Am. Chem. Soc.* **2001**, *123*, 7257.

(28) (a) Vetter, A. J.; Flaschenriem, C.; Jones, W. D. *J. Am. Chem. Soc.* **2005**, *127*, 12315. (b) Foley, N. A.; Lail, M.; Lee, J. P.; Gunnoe, T. B.; Cundari, T. R.; Petersen, J. L. *J. Am. Chem. Soc.* **2007**, *129*, 6765. (c) Menye-Biyogo, R.; Delpech, F.; Castel, A.; Pimienta, V.; Gornitzka, H.; Rivière, P. *Organometallics* **2007**, *26*, 5091.

(29) (a) Pimienta, V.; Lavabre, D.; Levy, G.; Micheau, J. C. *J. Phys. Chem.* **1995**, *99*, 14365. (b) Rivera-Islas, J.; Pimienta, V.; Micheau, J. C.; Buhse, T. *Biophys. Chem.* **2003**, *103*, 201.

(30) At this low [C$_6$H$_6$] to [**1**] ratio ([C$_6$H$_6$]/[**1**] = 2), mass balance was not fully maintained when only the main products shown in Scheme 5 were considered. Introduction of an additional decomposition pathway for intermediate A with rate constant k_5 afforded an acceptable fit for the data; if this decomposition process is not included in the fit, normalization of the concentrations is necessary for the experiment with [C$_6$H$_6$]/[**1**] = 2. Attempts to account for the decomposition process by invoking alternative elementary steps in the kinetic model did not solve this mass balance problem.

Table 1. Unimolecular Rate Constants and Bimolecular Rate Constant Ratios for the Reaction of **1** with C_6H_6 Giving **2** and **3** ($T = 323$ K)^a

	k_1/min^{-1} $(2.4 \pm 0.2) \times 10^{-2}$	k_{-2}/min^{-1} $(3 \pm 1) \times 10^{-3}$	k_3/min^{-1} $(1.53 \pm 0.06) \times 10^{-3}$	k_{-4}/min^{-1} $(8 \pm 2) \times 10^{-4}$	k_{-1}/k_2 0.3 ± 0.2	k_{-3}/k_4 1.2 ± 0.4	$k_5{}^b$/min^{-1} (18 ± 5)
normalized rate constant	1	0.13	0.06	0.03	0.3	1.2	750
normalized rate constant (DFT)	1	0.21	0.0003	0.01	0.5	0.37	

^{a} See Scheme 5 for significance of k_i. ^{b} See ref 30.
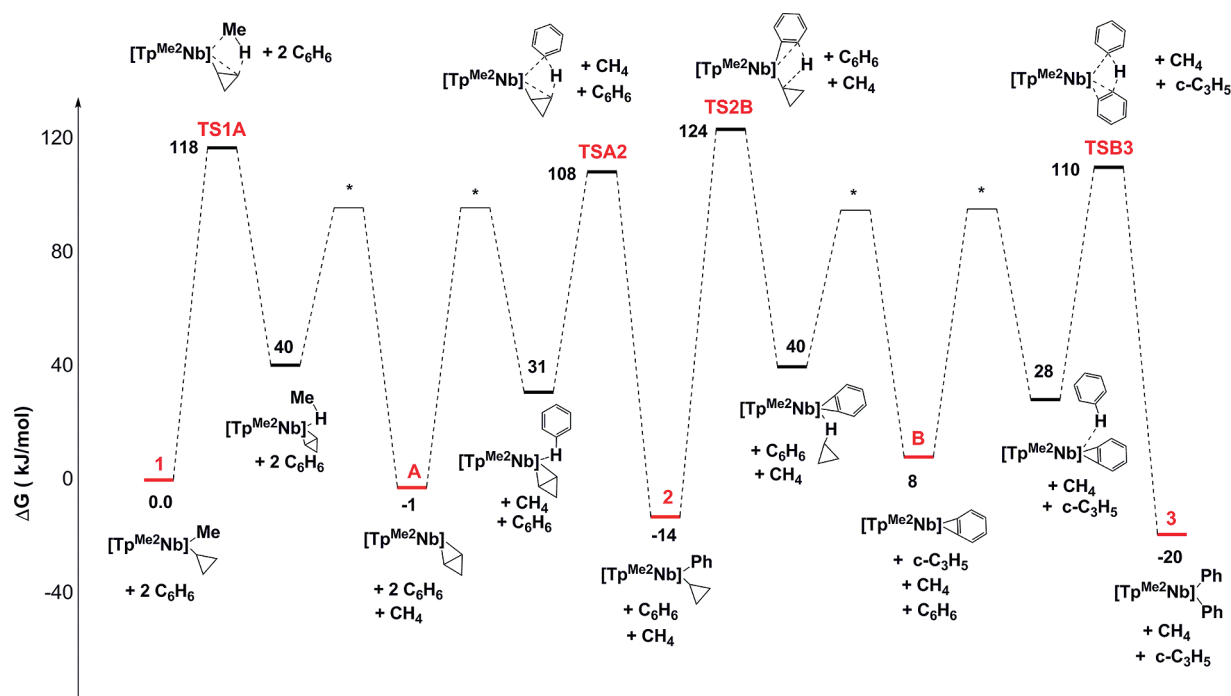
Figure 4. Free energy surface (including solvation) for the bond activation steps (kJ/mol, [Tp^{Me2}Nb] = Tp^{Me2}Nb(MeCCMe)). The energies of the transition states associated with formation/collapse of the σ complexes (labeled with an asterisk) have not been located.

unable to fully simulate the rates of reactions involving these species, k_{-1}, k_2, k_{-3}, and k_4. The ratios k_{-1}/k_2, and k_{-3}/k_4 can, however, be obtained. The concentrations of **1**, **2**, and **3** (normalized to initial concentration of **1**) are shown as a function of time in Figure 3 along with best fits obtained from the kinetic model. The corresponding kinetic parameters are collected in Table 1. The successful simultaneous fitting of data for all three sets of initial conditions confirms the validity of the model and allows the determination of the parameters with higher precision. Note that a unimolecular process k_5 accounting for decomposition of intermediate **A**, which proves to be significant only at low [C_6H_6]/[**1**] ratio, was introduced in the model to maintain mass balance.[30]

The values of the rate constants shown in Table 1 are generally consistent with the other experiments reported previously. The value of k_1 is similar to k_{obs} (note that the two experiments were performed at different temperatures), confirming the first step to be rate limiting. Moreover, the ratio $k_3/k_1 = 0.06$ is consistent with the empirical observation that β-H abstraction from **1** occurs at room temperature while elimination of cyclopropane from **2** requires elevated temperatures and longer times. From the common intermediate **2** there is little difference between the rates of β-H abstraction from a cyclopropyl ligand to give **A** (k_{-2}) or from a phenyl ligand to give **B** (k_3). As a result, the first step is reversible, allowing incorporation of more than one deuterium in the cyclopropyl group when C_6D_6 is used. The kinetic analysis also reveals that neither of the unsaturated intermediates, **A** or **B**, discriminates strongly between different substrates (benzene or hydrocarbon). Thus,

for **A**, $k_{-1}/k_2 = 0.3 \pm 0.2$, indicating a marginal kinetic preference for activation of benzene over methane and the rates of reactions with benzene and cyclopropane are identical within experimental error for **B** ($k_{-3}/k_4 = 1.2 \pm 0.4$). The fact that our kinetic model predicts that **A** is able to activate methane at all is a remarkable observation. We note however that this conclusion rests heavily on the persistence of small residual concentrations of **1** even at $t > 500$ s for the most dilute concentrations of benzene ([C_6H_6]/[**1**] = 2, left-hand graph), where accurate integration of the NMR peaks is challenging.

Reaction Mechanism: Computational Approach. Given that the experimental data summarized above and in our original communication indicate a complex mechanistic picture, we now report a series of calculations performed with density functional theory (M06). The aim is to confirm the structure of the key stationary points illustrated in Scheme 5 and to explore the origin of the unusual reactivity of the cycloalkene intermediate. The computed free energy surface (including solvation) for the conversion of **1** → **2** → **3** via intermediates **A** (a niobium cyclopropene species) and **B** (a benzyne complex) is shown in Figure 4, and structures of key stationary points are collected in Figure 5.[31] The general features of the two sections of the surface (**1** → **A** → **2** and **2** → **B** → **3**) are rather similar: in both cases hydrogen atom transfer leads to a weak van-der-Waals-type complex which decomposes via ligand loss to form **A** or **B**. Subsequent reaction with substrate is essentially the microscopic reverse, with formation of a weak complex preceding bond activation via transfer of H to the bound unsaturated ligand
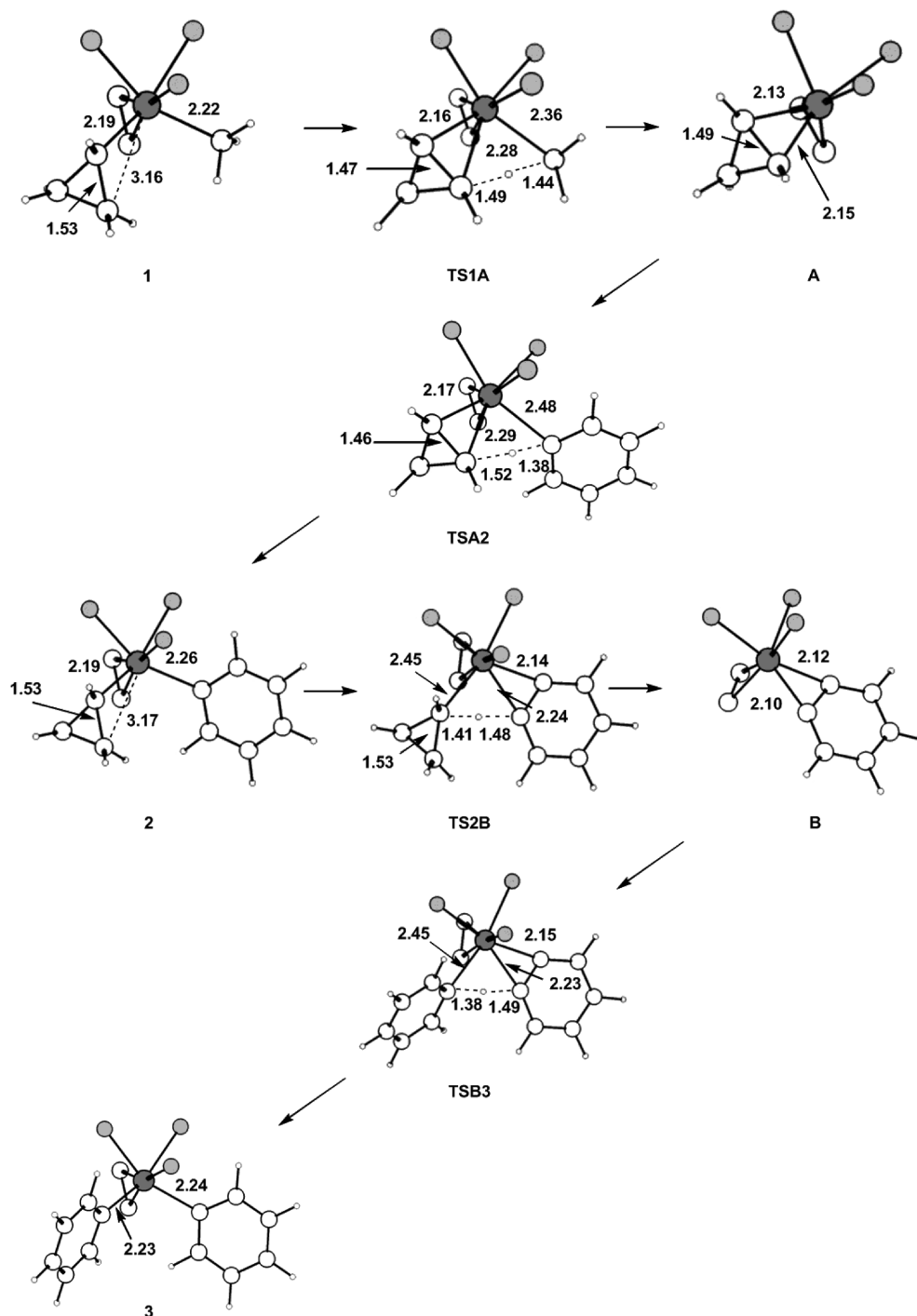
Figure 5. Optimized structures of the stationary points shown in Figure 4 (distances in Å).

(cyclopropene or benzyne). In the unsaturated cyclopropene and benzyne intermediates, **A** and **B**, the coordination geometry about the niobium center is approximately square pyramidal, with the two C−C units occupying mutually cis sites in the equatorial plane. The substantial elongation of the C=C double

bond in **A** compared to free cyclopropene (1.49 vs 1.29 Å) is indicative of a dominant metallacyclic resonance form for **A**, as noted in the crystal structure of **4**. Our calculations show that there are, in fact, two quite distinct but almost isoenergetic conformers of the cyclopropene complex **A**. In the first, the non-coordinated carbon is directed "up" into the wedge formed by two of the pyrazolyl arms of the Tp^{Me2} ligand, while in the other it points down. Reaction of the "down" conformer with C_6D_6 will yield the more abundant stereoisomer of **2-d_6** noted in Scheme 2, while the marginally less stable "up" conformer generates the minor stereoisomer. We also note at this point that the putative cyclopropylidene intermediate **A'** (isomeric to

(31) The known crystal structure of **2** offers a further opportunity to benchmark our chosen computational model (see Supporting Information). In this context, we simply note that all key features of the experimental structure are reproduced with good accuracy (computed Nb-C(phenyl) = 2.251 Å vs 2.254(4), Nb-C(cyclopropyl) = 2.185 Å vs 2.196(4) and C-C(cyclopropyl) = 1.500 Å, 1.528 Å and 1.483 Å vs 1.509(5), 1.523(6) and 1.482(6), respectively). For C-C agostic distortions in **1** and **2**, see ref 18.

A) that would arise from an α-H abstraction process lies 14 kJ/mol higher in energy. The relative instability of **A'** explains the absence of deuterium at the α- carbon in the reactions of **1** with benzene-d_6.

The thermodynamic balance between the different products and intermediates is very delicate with all five minima lying in a narrow window (28 kJ/mol). The thermodynamics of the C—H bond activation process are therefore rather insensitive to the precise nature of the bond (CH$_3$—H vs C$_3$H$_5$—H vs C$_6$H$_5$—H). The energies of the four key transition states connecting **1** and **3** via **A** and **B** also span only 16 kJ/mol, indicating that kinetic factors are similarly nondiscriminating, consistent with the complexity of the kinetic analysis presented above.[32] In each of the transition states the C—H—C unit is approximately linear (CHC angles >166°) with the hydrogen positioned symmetrically between the two carbon centers. The structural rearrangements highlighted in Figure 5 are very similar to those described by Legzdins and co-workers in a related study of molybdenum benzyne intermediates and are reminiscent of σ-bond metathesis processes. In **TS1A**, for example, the Nb—Cβ(cyclopropyl) and C(methyl)—H bonds are formed while Nb—C(methyl) and C(cyclopropyl)-H bonds are cleaved. Hall and co-workers[1d] have proposed that C—H bond activation transition states can be classified according to their molecular graphs, a σ-bond metathesis pathway being characterized by the absence of a bond critical point between the migrating hydrogen and the metal center. The molecular graphs of all four transition states display this pattern (an exemplary case, **TS1A**, is shown in Figure S1), with bond critical points linking the two carbon centers to both the migrating hydrogen and the niobium. The Mulliken charges on carbon and hydrogen change very little in the early stages of the reaction coordinate (**A** → **TS1A/TSA2** and **B** → **TS2B/TSB3**). The minimal redistribution of electron density contrasts with the C—H bond activation by Ti≡C and Ti≡C units reported recently by Mindiola and Baik,[17] where the polarity of the metal—carbon multiple bonds leads to significant charge transfer in the four-membered transition states.

In Table 1 we compare the computed normalized rate constants (obtained from the activation free energies assuming a constant pre-exponential factor in the Arrhenius equation) with those obtained from the fit to the experimental data. The computed results are remarkably consistent with experiment. For example, the calculated ratios $k_{-1}/k_2 = 0.5$ and $k_{-3}/k_4 = 0.37$ compare well with values of the 0.3 ± 0.2 and 1.2 ± 0.4 from the fitting of the kinetic data and confirm that neither **A** nor **B** discriminates strongly between substrates. The calculations also concur that β-H abstraction from a phenyl ligand by cyclopropyl (**2** → **B**) is slower than from cyclopropyl by methyl (**1** → **A**), although in this case the computed ratio is 2 orders of magnitude smaller than experiment.

Having established that our computed free energy surface is consistent with the measured kinetic data, we use it as a basis to explore the reasons why the η^2-cyclopropene intermediate, **A**, is able to participate in intermolecular C—H activation chemistry. As noted in the introduction, reactivity patterns of this type are almost unprecedented for η^2-alkene intermediates.

Clearly the strained C$_3$ ring will alter the properties of the alkene-based orbitals. To understand the impact on the free energy surface, we have conducted a parallel series of computations using ethyl, a typical acyclic alkyl ligand, in place of cyclopropyl, in the initial complex. Elimination of methane from Tp^{Me2}Nb(Me)(Et)(MeCCMe) (**1**$_{et}$) leads to Tp^{Me2}Nb(η^2-C$_2$H$_4$)(MeCCMe), **A**$_{et}$ the ethene analogue of **A**. The reaction in this case is exergonic (ΔG = −28 kJ/mol) in contrast to the corresponding reaction of **1** → **A** where ΔG = −1 kJ/mol. Thus, one effect of the C$_3$ ring is to reduce the thermodynamic driving force for the initial β-H abstraction step, stabilizing the alkyl complex. In this context, we note that we have been unable to synthesize analogues of **1** with any acyclic alkyl ligand bearing β hydrogens, presumably due to decomposition via β-H abstraction reactions of this type.

We emphasized in the introduction that alkene complexes of early transition metals (such as **A**$_{et}$) generally decompose rapidly via alkene loss. In the present context, alkene loss would represent a dead-end, as C—H activation could then only take place via an alternative (and presumably much higher energy) C—H oxidative addition pathway. Indeed, facile alkene loss seems to be the major obstacle to developing C—H activation chemistry in this class of complex. Given that the β-H abstraction process in **1** generates a cyclopropene complex, **A**, that is even less stable than **A**$_{et}$, a complex of a typical acyclic alkene, it is initially surprising that **A** apparently has a lifetime long enough to allow subsequent reaction with hydrocarbons. The answer to this paradox lies in the strength of the interaction between the alkene fragment and the niobium center in the intermediate. Despite the relative instability of **A** vs **A**$_{et}$ with respect to the alkyl precursors, the interaction between the metal center and the C=C π bond is actually considerably stronger in the former. Thus, the ligand exchange reaction **A** + C$_2$H$_4$ → **A**$_{et}$ + C$_3$H$_4$ is strongly endergonic (ΔG = +64 kJ/mol), clearly reflecting the ring strain in free cyclopropene that prepares the ligand for binding to the metal center. Consistent with the energetic data, the Nb—C bond lengths in **A** are 2.15 Å compared to 2.23 Å for **A**$_{et}$, while the Mulliken populations of +0.9 (Nb) and −0.31 (C) in **A** vs +0.72 and −0.22 in **A**$_{et}$ reflect the greater charge transfer involved in the formation of the Nb-(cyclopropene) bond. Thus, the unique reactivity of the cyclopropyl system, **1**, arises from the fact that the **A** intermediate is stabilized toward dissociation of the alkene, allowing the C—H activation processes discussed above to compete with decomposition pathways arising from ligand loss. The superior coordination of cyclopropene with respect to other more conventional olefins is directly related to its geometric strain.

Summary and Conclusions

We have shown that the niobium methyl cyclopropyl complex, **1**, undergoes decomposition via an unusual β-H abstraction pathway to generate an unsaturated η^2-bound cyclopropene intermediate, **A**. This species can be trapped either by pyridine or by acetone and can react with benzene, via activation of a C—H bond, to generate a cyclopropyl phenyl species, **2**. **2** can itself undergo β-H abstraction to generate an η^2-benzyne intermediate, **B**, that can activate a further molecule of benzene to generate a diphenyl species. The β-H abstraction/activation transition states connecting A and B to their respective substrates and products are typical (both structurally and electronically) of σ-bond metathesis pathways, with the migrating hydrogen atom positioned approximately at the center of a near-linear C—H—C array. A detailed analysis of the reaction

---

(32) We note at this point that we have been unable to locate transition states connecting any of **1**, **2**, **3**, **A** or **B** to the van-der-Waals complexes described above; this is unsurprising because, as noted by Baik and co-workers, their properties are most likely to be dominated by entropic rather than enthalpic factors. We do not anticipate that barriers to coordination/de-coordination of the hydrocarbon substrate will exceed those associated with C-H bond activation.

kinetics, along with a survey of the computed free energy surface, suggests that the two unsaturated intermediates, **A** and **B**, are rather unselective, reacting with aliphatic or aromatic C−H bonds with approximately equal rates.

The activation of C−H bonds by an η^2-alkene species represents a highly unusual reaction pathway — the majority of known examples with hydrocarbon ligands occur instead via alkylidenes generated by α-C-H abstraction. The unusual reactivity pattern in the case of **1** appears to stem from the ring strain in the cyclopropyl ligand which strengthens the Nb-(C≡C) bonding in the η^2-alkene, preventing decomposition by alkene loss. We have noted previously that the structure of **1** shows evidence for an α-C-C agostic interaction in the ground state, the origins of which undoubtedly also lie in the ring strain in the three-membered ring. The extent to which the two phenomena, ground-state α-C-C agostic bonding and efficient C−H bond activation, are directly correlated remains to be established. What is indisputable is that this system provides a remarkable example of how modification of a ligand can tune kinetic and thermodynamic factors to induce unusual reactivity patterns.

Experimental Section

All experiments were carried out under a dry argon atmosphere using either Schlenck tube or glovebox techniques. Diethylether were obtained after refluxing purple solutions of Na/benzophenone under argon. Benzene, pentane, cyclohexane, pyridine, and dichloromethane were dried by refluxing over CaH₂ under argon. Deuterated NMR solvents were dried over molecular sieves, degassed by freeze−pump−thaw cycles, and stored under argon. ¹H and ¹³C NMR spectra were obtained on Bruker AM 250, DPX 300, AMX 400, Avance 300 or 500 spectrometers at room temperature unless otherwise stated. Only pertinent $^1J_{CH}$ are quoted in the ¹³C spectra. Tp^{Me2}NbCl(*c*-C₃H₅)(MeC≡CMe) was prepared according to a published procedure.[33]

Tp^{Me2}NbMe(*c*-C₃H₅)(MeC≡CMe) (1). Tp^{Me2}NbCl(*c*-C₃H₅)-(MeC≡CMe) (0.40 g, 0.77 mmol) was dissolved in a mixture diethyl ether (15 mL) and pentane (35 mL), and cooled to −20 °C. Methyl lithium (1.6 M, 0.6 mL, 0.96 mmol) was added dropwise over a period of 2−3 min. The color of the solution gradually changed from orange to yellow brown as the temperature slowly rose to 0 °C. After about 4 h, air was briefly admitted into the flask for ca. 5 min by removing the septum under static vacuum. The solution turned yellow. The solvent was stripped off and the residue was extracted with pentane. The slurry was filtered through a pad of Celite to give a clear yellow solution, which was slowly concentrated under a vacuum to induce crystallization. A bright yellow microcrystalline powder was isolated, rapidly rinsed with cold pentane, and dried under a vacuum (0.31 g, 0.62 mmol, 80%). The complex must be stored below 0 °C. For **1**: ¹H NMR (500 MHz, benzene-*d₆*, 283 K) δ 5.96, 5.83, 5.65 (all s, 1 H each, Tp^{Me2}C*H*), 3.10, 2.45 (both s, C*H₃*C≡), 2.78, 2.38, 2.32, 2.24, 2.19, 1.89 (all s, 3 H each, Tp^{Me2}C*H₃*), 1.60 (m, 1 H, *c*-C₃H₅ α), 1.34 (s, 3H, NbC*H₃*), 0.93, 1.37, 1.82 (m, 1:2:1 H, *c*-C₃H₅ β). ¹³C NMR (125.8 MHz, benzene-*d₆*, 283 K) δ 241.7, 234.8 (Me*C*≡), 151.8, 151.4, 150.2, 143.7, 143.4, 143.3 (Tp^{Me2}C*C*H₃), 107.68, 106.9, 106.7 (Tp^{Me2}*C*H), 62.6 (br d, $^1J_{CH}$ 139 Hz, Nb*C*α*H*), 48.7 (br q, $^1J_{CH}$ 119 Hz, Nb*C*H₃), 21.9, 19.2 (*C*H₃C≡), 20.3, 11.5 (both t, $^1J_{CH}$ 160, 156 Hz, *C*βH₂, *C*β'H₂), 15.5, 15.1, 14.2, 12.8, 12.6, 12.5 (Tp^{Me2}C*H₃*). Anal. Calcd for C₂₃H₃₆BN₆Nb: C, 55.22; H, 7.25; B, 2.16; N, 16.80. Found: C, 55.66; H, 7.33; N, 16.43.

Tp^{Me2}NbPh(*c*-C₃H₅)(MeC≡CMe) (2). Tp^{Me2}NbMe(*c*-C₃H₅)-(MeC≡CMe) (0.250 g, 0.50 mmol) was dissolved in benzene (10 mL) and stirred for ca. 40 h. The color of the solution changed from yellow to yellow brown. The solvent was evaporated to

dryness. The residue was extracted with pentane, and the slurry was filtered through a pad of Celite to give a clear yellow solution that was slowly concentrated under vacuum to induce crystallization. A bright yellow microcrystalline powder was isolated, rinsed with cold pentane and dried under a vacuum (0.21 g, 0.37 mmol, 74%). For **2**: ¹H NMR (500 MHz, benzene-*d₆*, 283 K) δ 7.04 (t, 1H, *p*-C₆H₅), 5.74, 5.72, 5.59 (all s, 1H each, Tp^{Me2}C*H*), 2.98, 2.27 (both s, C*H₃*C≡), 2.25, 2.18, 2.15, 2.13, 1.85, 1.36 (all s, 3 H each, Tp^{Me2}C*H₃*), 2.22 (m, 1 H, *H₇'*), 2.09 (m, 1 H, *H₅*), 1.63 (m, 1 H, *H₆'*), 1.42 (m, 1 H, *H₆*), 0.90 (m, 1 H, *H₇*). *ortho* and *meta* phenyl protons are not observed at this temperature due to restricted rotation about the NbC₆H₅ bond. ¹³C NMR (125.8 MHz, benzene-*d₆*, 283 K) δ 242.2, 239.4 (Me*C*≡C), 192.1 (Nb-α-*C₆H₅*), 153.1, 151.0, 150.8, 144.0, 143.5, 143.3 (Tp^{Me2}C*C*H₃), 137.4, 126.3, 125.6 (*C₆H₅*), 107.5, 107.1, 107.0 (Tp^{Me2}*C*H), 71.9 (br d, $^1J_{CH}$ 142 Hz, Nb*C*α*H*), 22.4, 19.2 (*C*H₃C≡), 22.1, 12.4 (both t, $^1J_{CH}$ 159, 162 Hz, *C*βH₂, *C*β'H₂), 15.3, 15.1, 14.6, 12.8, 12.7, 12.6 (Tp^{Me2}C*H₃*). Anal. Calcd for C₂₈H₃₈BN₆Nb: C, 59.81; H, 6.81; N, 15.00. Found: C, 60.12; H, 6.93; N, 14.71.

Tp^{Me2}NbPh₂(MeC≡CMe) (3). Tp^{Me2}NbMe(*c*-C₃H₅)(MeC≡CMe) (0.250 g, 0.50 mmol) was heated in benzene (10 mL) at 50 °C for 48 h. The color of the solution changed from yellow to orange. The solvent was evaporated to dryness. The residue was then extracted with pentane, and the slurry was filtered through a pad of Celite to give a clear orange solution which was slowly concentrated under vacuum to induce crystallization. A bright orange microcrystalline powder was isolated, rinsed with cold pentane and dried under a vacuum (0.230 g, 0.385 mmol, 74%). For **3**: ¹H NMR (500 MHz, dichloromethane-*d₂*) δ 6.99 (t, 1 H, *p*-C₆H₅), 5.90, 5.62 (both s, 2:1 H, Tp^{Me2}C*H*), 2.87 (br s, 6 H, C*H₃*C≡), 2.59, 2.58, 1.53, 0.42 (all s, 3:6:6:3 H, Tp^{Me2}C*H₃*); (500 MHz, dichloromethane-*d₂*, 213 K) δ 8.50, 6.19 (both t, ^3J 5 Hz, 1 H, *o*-C₆H₅), 7.25, 6.67 (both t, ^3J 5 Hz, 1 H, *m*-C₆H₅), 6.97 (d, ^3J 5 Hz, 1 H, *p*-C₆H₅), 5.90, 5.58 (both s, 2:1 H, Tp^{Me2}C*H*), 3.32, 2.36 (both s, 1 H, C*H₃*C≡), 2.54, 1.50, 0.21 (all s, 9:6:3 H, Tp^{Me2}C*H₃*). ¹³C NMR (125.8 MHz, dichloromethane-*d₂*, 213 K) δ 250.1, 249.1 (Me*C*≡), 197.1 (Nb-α-*C₆H₅*), 152.6, 150.4, 144.4, 143.9 (Tp^{Me2}C*C*H₃), 137.0, 134.7, 126.3, 125.8, 126.0 (*C₆H₅*), 106.8, 107.1, 106.6 (Tp^{Me2}*C*H), 24.1, 19.3 (*C*H₃C≡), 14.8, 12.8, 13.3, 12.5 (Tp^{Me2}C*H₃*). Anal. Calcd for C₃₁H₃₈BN₆Nb: C, 62.22; H, 6.40; B, 1.81; N, 14.04. Found: C, 61.52; H, 6.65; N, 13.71.

Tp^{Me2}Nb(NC₅H₅)(η^2-C₃H₄)(MeC≡CMe) (4). Tp^{Me2}NbMe(*c*-C₃H₅)(MeC≡CMe) (0.600 g, 1.20 mmol) was dissolved in pentane (30 mL) and pyridine (480 mg, 6.1 mmol) was added. The yellow solution rapidly became dark green. The solution was allowed to stand still for 4 days. A black green supernatant was then filtered off. The remaining dark green powder was washed with cold pentane (3 × 1 mL) and dried under a vacuum to leave 590 mg of **4** (1.06 mmol, 85%). Single crystals suitable for an X-ray analysis were obtained following the same procedure from a more concentrated solution in pyridine (2.5 mol·L⁻¹). ¹H NMR (400.1 MHz, cyclohexane-*d₁₂*) δ 8.47 (br, 2H, *o*-C₅H₅N), 7.46 (t, 1H, *p*-C₅H₅N), 6.92 (br, 2H, *m*-C₅H₅N), 5.89, 5.53, 5.42 (all s, 1H each, Tp^{Me2}C*H*), 2.83 (t, 1H, NbC*H*CHCH₂), 2.60 (overlaps, 1H, NbCHC*H*CH₂), 2.60, 2.01 (br s, 3H each, C*H₃*C≡), 2.48, 2.45, 2.42, 2.41, 1.55, 0.92 (all s, 3 H each, Tp^{Me2}C*H₃*), 1.62 (q, 1 H, NbCHCHC*H₂*), −0.20 (d, 1 H, NbCHCHC*H₂*), *o*-protons of pyridine are not observed at this temperature due to restricted rotation about the Nb-(C₅H₅N) bond. ¹³C NMR (100.6 MHz, cyclohexane-*d₁₂*, 298 K) δ 209.1, 206.9 (Me*C*≡C), 155.2 (very br, *o*-C₅H₅N), 153.9, 150.2, 149.0, 142.5, 141.8, 141.6 (Tp^{Me2}C*C*H₃), 135.1 (s, *m*-C₅H₅N), 121.7 (s, *p*-C₅H₅N), 106.7, 106.6, 105.9 (Tp^{Me2}*C*H), 74.5 (br d, $^1J_{CH}$ = 173.3 Hz, Nb*C*HCHCH₂), 68.4 (br d, $^1J_{CH}$ = 167.8 Hz, NbCH*C*HCH₂), 27.3 (dd, $^1J_{CH}$ = 147.0, 174.0 Hz, NbCHCH*C*H₂), 17.9, 16.7 (*C*H₃C≡), 16.4, 13.7, 13.3, 12.7, 12.5, 12.2 (Tp^{Me2}C*H₃*). ¹H NMR (500.3 MHz, dichloromethane-*d₂*, 193 K) δ 10.67 (br s, 1H, *o*-C₅H₅N), 7.68 (br s, 1H, *p*-C₅H₅N), 7.47, 6.75 (both br s, 1H, *m*-C₅H₅N), 6.50 (s, 1H, *o*-C₅H₅N), 6.12, 5.70, 5.60 (all s, 1H each, Tp^{Me2}C*H*), 2.70, 2.25 (both br s, 1H, NbC*H*CH*C*H₂), 2.63, 2.06

(33) Jaffart, J.; Cole, M. L.; Etienne, M.; Reinhold, M.; McGrady, J. E.; Maseras, F. *Dalton Trans.* **2003**, 4057.

(both s, 3H each, CH_3C≡), 2.55, 2.53, 2.46, 2.43, 1.45, 0.88 (all s, 3 H each, Tp^{Me2}CH_3), 1.45 (overlaps, br s, 1 H, NbCHCHCH$_2$), −0.48 (br s, 1 H, NbCHCHCH$_2$). ^{13}C{^{1}H} NMR (125.1 MHz, dichloromethane-d_2, 193 K) δ 214.7, 207.1 (MeC≡), 158.2, 151.4 (o-C$_5$H$_5$N), 154.2, 150.8, 150.0, 144.5, 144.3, 143.8 (Tp^{Me2}CCH$_3$), 137.0 (p-C$_5$H$_5$N), 123.7, 122.5 (m-C$_5$H$_5$N), 107.2, 107.0, 106.8 (Tp^{Me2}CH), 70.6, 66.6 (br s, NbCHCHCH$_2$), 27.1 (br s, NbCH-CHCH$_2$), 19.4, 18.3 (CH_3C≡), 17.0, 14.8, 14.6, 14.0, 13.7, 13.5 (Tp^{Me2}CH_3). Anal. Calcd for C$_{27}$H$_{37}$BN$_7$Nb: C, 57.56; H, 6.62; N, 17.40; Found: C, 57.45; H, 6.88; N, 17.29.

Tp^{Me2}NbO(C$_{13}$H$_{22}$O) (5). Tp^{Me2}Nb(c-C$_3$H$_5$)(CH$_3$)(MeC≡CMe) (0.103 g, 0.21 mmol) was dissolved in cyclohexane (5 mL) and acetone (34 μL, 0.46 mmol) was added dropwise. After six days at room temperature, the solution was evaporated to dryness. The residue was extracted with pentane (5 mL) and filtered through a pad of Celite. A dark powder was obtained after evaporation. This powder is composed of a mixture of compounds of which **5** was vastly major as judged by ^{1}H NMR. No efforts were made to get an analytical sample. Single crystals suitable for X-ray diffraction were obtained from a concentrated benzene-d_6 solution. For **5**: ^{1}H NMR (500 MHz, benzene-d_6, 293 K) δ 5.62, 5.54, 5.31 (all s, 1H, Tp^{Me2}CH), 5.56 (t, $^3J_{HH}$ = 7.5 Hz, 1H, HC=C(CH$_3$)$_2$), 4.78 (dd, $^3J_{HH}$ = 5.9 Hz, 1H, NbOCCH), 2.53 (m, 2H, CH_2CH=), 2.64, 2.52, 2.38, 2.16, 2.12, 2.03 (all s, 3H, Tp^{Me2}CH_3), 2.11, 1.15 (both s, 3H, OC(CH_3)$_2$), 1.99 (s, 3H, NbC=CCH_3), 1.72, 1.66 (s, 3H, =C(CH_3)$_2$), 1.59 (s, 3H, NbCCH_3). ^{13}C NMR (125 MHz, benzene-d_6) δ 185.9 (NbC), 153.2, 152.1, 151.6, 145.8, 144.0, 143.5 (Tp^{Me2}CCH$_3$), 141.7 (NbC=C), 130.5 (=C(CH$_3$)$_2$), 126.3 (CH=C(CH$_3$)$_2$), 106.7, 106.3, 106.2 (Tp^{Me2}CH), 91.9 (CO), 64.1 (NbOCCH), 29.2 (CH$_2$CH=), 28.3, 27.8, 25.8, 24.2 (C(CH$_3$)$_2$)), 21.8 (NbCCH$_3$), 17.5 (NbC=CCH$_3$), 14.9, 14.2, 14.2, 12.5, 12.4, 12.0 (Tp^{Me2}CH_3). When the reaction was carried out with acetone-d_6, **5-d_{12}** was obtained with ^{1}H NMR signals of **5** at δ 2.11, 1.15, 1.72, and 1.66 were not observed.

Tp^{Me2}Nb(PMe$_3$)($η^2$-C$_6$H$_4$)(MeC≡CMe) (6). Tp^{Me2}NbPh$_2$(MeC≡CMe) (0.037 g, 0.06 mmol) was introduced in a screw-cap NMR tube and dissolved in 0.4 mL of C$_6$D$_{12}$. PMe$_3$ (50 μL, 0.049 mmol) was added, and the solution was heated at 50 °C for 5 h. 0.5 mL of pentane was added dropwise and the solution was filtered through a pad of Celite. The solution was pumped to dryness and the resulting powder was dissolved in cyclohexane-d_{12} for analysis. No efforts were made to get an analytical sample, see text and **7**. For **6**: ^{1}H NMR (300 MHz, cyclohexane-d_{12}, 298K) δ 7.97, 7.45 (both d, $^3J_{HH}$ = 6.5 Hz, CHC≡), 7.13, 6.95 (both t, $^3J_{HH}$ = 6.5 Hz, CHCC≡), 5.87, 5.61, 5.37 (all s, 3H, Tp^{Me2}CH), 2.59, 2.17 (both s, 3H, CH_3C≡), 2.67, 2.38, 2.34, 2.31, 1.78, 0.70 (all s, 3H, Tp^{Me2}CH_3) 1.04 (d, $^2J_{PH}$ = 6.7 Hz, 9H, PCH_3), ^{13}C{^{1}H} NMR (75.48 MHz, cyclohexane-d_{12}, 298 K) δ 207.0 (d, $^2J_{PC}$ = 20 Hz), 202.5, 185.4 (d, $^2J_{PC}$ = 30 Hz),180.2 (MeC'), 152.5, 152.3, 150.6, 143.3, 143.2, 142.4 (Tp^{Me2}CCH$_3$), 130.8 (br d, $^4J_{PC}$ = 4 Hz, CHC≡), 129.3 (s, CHC≡), 128.5, 126.2, (s, CHCHC'), 107.4, 107.1, 105.9 (Tp^{Me2}CH), 20.6, 18.1 (s, CH$_3$−C≡), 17.4 (d, $^2J_{PC}$ = 14.3 Hz, P(CH$_3$)$_3$) 16.2, 14.9, 12.8, 12.6, 12.3, 12.3 (Tp^{Me2}CH_3).

Tp^{Me2}Nb(CO)($η^2$-C$_6$H$_4$)(MeC≡CMe) (7). Tp^{Me2}NbMe(c-C$_3$H$_5$)-(MeC≡CMe) (0.557 g, 1.11 mmol) was heated in benzene (5 mL) at 50 °C for 48 h. The color of the solution changed from yellow to orange. PMe$_3$ (0.25 mL, 2.45 mmol) of was added dropwise and the solution was stirred at 50 °C for 9 h. CO was then gently bubbled through the solution at room temperature for 1 h producing a dark precipitate. The solvent was removed under a vacuum and the precipitate was washed with 5 × 8 mL of pentane. A powder was isolated and dried under a vacuum (0.172 g, 0.31 mmol, 30%). Crystals was obtained by gas phase diffusion of hexane into a toluene solution. For **7**: ^{1}H NMR (300 MHz, benzene-d_6, 298 K) δ 8.47 (dd, $^3J_{HH}$ = 7.0 Hz, $^4J_{HH}$ = 0.7 Hz, 1H, ≡CCH), 7.64 (dd, $^3J_{HH}$ = 6.5 Hz, $^4J_{HH}$ = 0.5 Hz, 1H, ≡CH), 7.51 (dd, $^3J_{HH}$ = 6.7 Hz, $^3J_{HH}$ = 6.7 Hz, 1H, ≡CCCH), 7.24 (dd, $^3J_{HH}$ = 6.5 Hz, $^3J_{HH}$ = 6.5 Hz, 1H, ≡CCCH), 6.13, 5.39, 5.10 (all s, 1H, Tp^{Me2}CH), 2.71, 2.06 (all s, 3H, CH_3C≡), 2.55, 2.40, 2.06, 1.97, 1.87, 1.33

(all s, 3H, Tp^{Me2}CH_3). ^{13}C{^{1}H} NMR (75 MHz, benzene-d_6, 298 K) δ 220.7 (br s, CO), 180.0, 177.3 (both MeC≡), 170.3, 166.6 (both C=CCH), 153.1, 151.2, 150.3, 143.9, 143.8, 143.5 (Tp^{Me2}CCH$_3$), 131.9, 129.2 (br d, $^1J_{CH}$ = 155 Hz, CHCC≡), 130.6, 124.9 (dd, $^1J_{CH}$ = 162 Hz, $^2J_{CH}$ = 8 Hz, CHC≡), 107.5, 107.0, 106.8 (Tp^{Me2}CH), 16.6, 16.1 (CH_3C≡), 16.4,14.8, 14.2, 13.1, 12.6, 12.6 (Tp^{Me2}CH_3). IR (solid state) $ν_{C=O}$ 1909 cm$^{−1}$. Anal. Calcd for C$_{31}$H$_{38}$BN$_6$Nb: C, 56.96; H, 5.88; N, 15.33. Found: C, 56.60; H, 5.95; N, 14.85.

Kinetics of the Reaction between 1 and Benzene and/or Benzene-d_6. Under argon, a weighted amount of **1** (ca. 10$^{−4}$ mmol) was introduced in a screw-cap NMR tube. Cyclohexane-d_{12} was added so that the total volume (cyclohexane-d_{12} + arene) was 0.5 mL. The appropriate amount of benzene (and/or benzene-d_6) was added dropwise with a microsyringue. The tube was then placed in the preheated NMR probe of the AM250 or AV300 spectrometer. Acquisitions of ^{1}H NMR spectra started 10 min later to allow temperature equilibration. Each acquisition was composed of eight scans with a 13 s delay between scans (total acquisition time 2 min). The kinetic isotope effect was obtained from a competition experiment were a 1/1 mixture of benzene/benzene-d_6 was allowed to react with **1** in a similar manner. Two experiments gave k_H/k_D = 4.0 ± 0.5.

Simulation and Data Fitting. Experimental NMR data were collected according to the procedure described above. A homemade program SA was used to simultaneously fit the data from three different kinetic runs ([C$_6$H$_6$]/[**1**] = 2, 6, 31). Differential equations (see Supporting Information) were integrated numerically using a semi-implicit Runge−Kutta method. The parameters were fitted automatically using an iterative algorithm of the Powell type, designed to minimize the residual quadratic error $E = \sum_j \sum_i [c_{ij} - e_{ij}]^2/(n \cdot N)$ where c_{ij} and e_{ij} are the computed and experimental values of concentrations respectively, n is the number of data point in a given run, and N is the number of runs (nine in this case). Errors on the resulting rate constants and rate constant ratios were obtained by assuming a variation of the residual error of 10%. Because of biased mass balance originating from decomposition of intermediates, a decomposition pathway modeled by a first-order process was added to the kinetic scheme (see text and Supporting Information).

X-ray Crystallography. Data for **4** were collected at 180 K on a Bruker Kappa Apex II diffractometer using a graphite-mono-chromated Mo−Kα radiation (λ = 0.71073 Å) and equipped with an Oxford Cryosystems Cryostream Cooler Device. The final unit cell parameters have been obtained by means of least-squares refinement performed on a set of 3359 well measured reflections. Light yellow crystal, C$_{27}$H$_{37}$BN$_7$Nb.C$_5$H$_5$N, FW 642.46 g·mol$^{−1}$, triclinic, $P\bar{1}$, a = 8.3166(8), b = 10.2440(10), c = 18.5583(17) Å, α = 93.377(3), β = 93.939(4), γ = 93.022(4)°, V = 1572.0(3) Å^3, T = 180(2) K, Z = 2, final R indices [I >2σ(I)]: R_1 = 0.0624, wR_2 = 0.1344, goodness-of-fit on F^2: 1.083.

Data for **5** were collected at 180 K on a IPDS STOE diffracto-meter using a graphite-monochromated Mo−Kα radiation (λ = 0.71073 Å) and equipped with an Oxford Cryosystems Cryostream Cooler Device. The final unit cell parameters have been obtained by means of least-squares refinement performed on a set of 8000 well measured reflections. Light yellow crystal, C$_{28}$H$_{44}$BN$_6$NbO$_2$; FW 600.41 g·mol$^{−1}$, monoclinic, $C2/c$, a = 31.593(3), b = 10.0459(6), c = 27.465(2) Å, β = 113.036(10) °, V = 8021.8(11) Å^3, T = 180(2) K, Z = 8, Final R indices [I > 2σ(I)]: R_1 = 0.0505, $wR2$ = 0.1319, goodness-of-fit on F^2: 0.867.

Data for **7** were collected at 180 K on an Xcalibur Oxford Diffraction diffractometer using a graphite-monochromated Mo−Kα radiation (λ = 0.71073 Å) and equipped with an Oxford Instrument Cooler Device. The final unit cell parameters have been obtained by means of a least-squares refinement on a set of 5964 well measured reflections. Light yellow crystal, C$_{26}$H$_{32}$BN$_6$NbO; FW 548.3 g·mol$^{−1}$, monoclinic, $P\,1\,21\,1$, a = 8.2075(5), b = 15.1721(9), c = 10.3794(6) Å, β = 93.729(5)°, V = 1289.76(13)

$Å^3$, $T = 180(2)$ K, $Z = 2$, final R indices [$I > 2\sigma(I)$]: $R_1 = 0.0302$, $wR_2 = 0.0508$, goodness-of-fit on F^2: 0.927.

All structures have been solved by direct methods using SIR92,[34] and refined by means of least-squares procedures on F^2 with the aid of the program SHELXL97[35] included in the software package WinGX version 1.63.[36] The Atomic Scattering Factors were taken from the International Tables for X-ray Crystallography.[37] All hydrogen atoms were geometrically placed and refined by using a riding model. All non-hydrogen atoms were anisotropically refined, and in the last cycles of refinement a weighting scheme was used, where weights were calculated from the following formula: $w = 1/[\sigma^2(F_o^2) + (aP)^2 + bP]$ where $P = (F_o^2 + 2F_c^2)/3$. Plots of molecular structures were performed with the program ORTEP32[38] with 30% probability displacement ellipsoids for non-hydrogen atoms.

Computational Details. Calculations were performed at the DFT level with the M06 functional[39] as implemented in Gaussian09.[40] Nb was described using the Stuttgart/Dresden RECP (SDD) and its associated basis set for the outer electrons.[41] The standard 6-31G(d) basis set was used for all other atoms.[42] The smd method, as implemented in Gaussian09, was used to incorporate solvation effects.[43] The structures of stationary points and transition states were fully optimized without any symmetry restriction. Transition states were identified by having one imaginary frequency.

Supporting Information Available: Full refs 1k and 40, kinetic model used for data simulation in Figure 3 and Table 1, optimized Cartesian coordinates for all stationary points reported in Figure 5, a molecular graph of **TS1A**, and CIF files for the X-ray structures of **4**, **5**, and **7**. This material is available free of charge via the Internet at http://pubs.acs.org.

JA1061505

(34) Altomare, A.; Cascarano, G.; Giacovazzo, C.; Guagliardi, A. *J. Appl. Crystallogr.* **1993**, *26*, 343.

(35) Sheldrick, G. M. *SHELX97 [includes SHELXS97, SHELXL97, CIFT-AB] - Programs for Crystal Structure Analysis (Release 97−2)*; Institüt für Anorganische Chemie der Universität: Göttingen, Germany, 1998.

(36) Farrugia, L. *J. Appl. Crystallogr.* **1999**, *32*, 837.

(37) *International Tables for X-ray Crystallography*; Kynoch Press: Birmingham, England, 1974; Vol *IV*.

(38) Farrugia, L. J. *J. Appl. Crystallogr.* **1997**, *30*, 565.

(39) (a) Zhao, Y.; Truhlar, D. G. *Acc. Chem. Res.* **2008**, *41*, 157. (b) Zhao, Y.; Truhlar, D. G. *Theor. Chem. Acc.* **2008**, *120*, 215.

(40) Frisch, M. J.; et al. *Gaussian 09*; Gaussian Inc.: Wallingford, CT, 2009.

(41) Andrae, D.; Häussermann, U.; Dolg, M.; Stoll, H.; Preuss, H. *Theor. Chim. Acta* **1990**, *77*, 123.

(42) Francl, M. M.; Pietro, W. J.; Hehre, W. J.; Binkley, J. S.; Gordon, M. S.; Defrees, D. J.; Pople, J. A. *J. Chem. Phys.* **1982**, *77*, 3654.

(43) Marenich, A. V.; Cramer, C. J.; Truhlar, D. G. *J. Phys. Chem. B* **2009**, *113*, 6378.